ISSN: 2476-6909; Modares. Mech. Eng. *2026;26(04):283-292.*

Modares Mechanical Engineering

DOI: 10.48311/mme.2025.116433.0
journal homepage: mme.modares.ac.ir

Effect of Centrifuge Table Rotation on Two-DOF Pedestal Dynamics in Acceleration Simulations

Seyed Hesameddin Madani*, Shahryar Zare

Department of Mechanical Engineering, Iranian Research Organization for Science and Technology (IROST), Tehran, Iran

ARTICLE INFO

Article Type
Original Research

Article History
Received: August 01, 2025
Revised: November 04, 2025
Accepted: December 15, 2025
ePublished: February 16, 2026

ABSTRACT

In this paper, for the first time, the effect of centrifuge table rotation on the dynamic behavior of a two-dimensional (two degrees of freedom) base in tracking systems is investigated and analyzed. While most previous studies have primarily focused on the effects of linear acceleration or vibrations, the present research employs a dynamic modeling approach based on Lagrange's formulation to demonstrate that the rotation of the centrifuge table can impose significant additional torques on the gimbal axes (Pitch and Yaw). To this end, the dynamic equations are derived for two key configurations: alignment and orthogonality of the Yaw axis relative to the centrifuge rotation axis. Additionally, the influence of the rotating system's center of mass location is examined. The findings reveal that it is not solely the centrifugal acceleration, but the centrifuge table's rotation itself that can independently generate detrimental torques. This phenomenon may lead to substantial errors in the estimation of the motor torque requirements, which have previously been overlooked in analytical studies.

Keywords: Centrifugal rotation, Moment of inertia matrix, Maximum torque

How to cite this article
Madani S.H, Zare Sh, Effect of Centrifuge Table Rotation on Two-DOF Pedestal Dynamics in Acceleration Simulations. Modares Mechanical Engineering; *2026;26(04):283-292.*

*Corresponding author's email: hesam_madani@irost.ir
*Corresponding ORCID ID: 0009-0006-5481-5231

شاپا: ۷۹۰۹-۲۴۷۶؛ مهندسی مکانیک مدرس. ۲۹۲-۲۸۳:(۰۴)۲۶;۱۴۰۵

مهندسی مکانیک مدرس

DOI: 10.48311/mme.2025.116433.0

صفحه اصلی مجله: mme.modares.ac.ir

اثر چرخش میز سانتریفیوژ بر دینامیک پایهٔ دو درجه آزادی در شبیه‌سازی‌های شتاب

سید حسام الدین مدنی*، شهریار زارع

گروه مهندسی مکانیک، سازمان پژوهش های علمی و صنعتی ایران، تهران، ایران

اطلاعات مقاله

نوع مقاله
مقاله پژوهشی

تاریخچه مقاله
دریافت: ۱۴۰۴/۰۵/۱۰
بازنگری: ۱۴۰۴/۰۸/۱۳
پذیرش: ۱۴۰۴/۰۹/۲۴
ارائه آنلاین: ۱۴۰۴/۱۱/۲۷

چکیده

در این مقاله، برای نخستین بار، اثر چرخش میز سانتریفیوژ بر رفتار دینامیکی یک پایهٔ دوبعدی (دارای دو درجه آزادی) در سامانه‌های رهگیری مورد بررسی و تحلیل قرار می‌گیرد؛ در حالی که اغلب مطالعات پیشین عمدتاً بر اثرات شتاب خطی یا ارتعاشات تمرکز داشته‌اند، پژوهش حاضر با بهره‌گیری از یک رویکرد مدل‌سازی دینامیکی مبتنی بر فرمول‌بندی لاگرانژ نشان می‌دهد که چرخش میز سانتریفیوژ می‌تواند گشتاورهای اضافی و قابل‌توجهی را بر محورهای گیمبال (Pitch) و (Yaw) اعمال کند؛ بدین منظور، معادلات دینامیکی برای دو پیکربندی کلیدی، یعنی هم‌راستایی و عمود بودن محور یاو نسبت به محور چرخش سانتریفیوژ، استخراج شده‌اند و علاوه بر این، تأثیر مکان مرکز جرم سامانهٔ در حال چرخش نیز مورد بررسی قرار گرفته است؛ نتایج نشان می‌دهند که نه‌تنها شتاب گریز از مرکز، بلکه خودِ چرخش میز سانتریفیوژ می‌تواند به‌طور مستقل موجب ایجاد گشتاورهای نامطلوب شود، پدیده‌ای که ممکن است به خطاهای قابل‌توجهی در برآورد نیازمندی‌های گشتاور موتور منجر شود؛ خطاهایی که پیش‌تر در مطالعات تحلیلی نادیده گرفته شده‌اند.

کلیدواژه‌ها: چرخش گریز از مرکز، ماتریس ممان اینرسی، حداکثر گشتاور

نحوه ارجاع به این مقاله

مدنی سید حسام الدین، زارع شهریار، اثر چرخش میز سانتریفیوژ بر دینامیک پایهٔ دو درجه آزادی در شبیه‌سازی‌های شتاب ، مهندسی مکانیک مدرس. ۲۹۲-۲۸۳:(۰۴)۲۶;۱۴۰۵

*پست الکترونیکی نویسنده عهده‌دار مکاتبات: hesam_madani@irost.ir

*شناسه ارکید نویسنده عهده‌دار مکاتبات: 0009-0006-5481-5231

1- Introduction

Stabilization of sensors such as infrared (IR), laser, or radar systems is of critical importance in various aerospace applications, including sensor-specific, actuation target tracking, and image processing [1, 2]. This capability is achieved through the implementation of a two-axis gimbal suspension system. A gyroscope is generally mounted on a rotating structure or the inner pedestal to measure angular velocities along two specified directions[3, 4]. These measurements are employed as feedback signals to control the torque actuators employed in the gimbals. The goal is to reduce external disturbances and maintain the inner pedestal aligned with the desired orientation. When the disturbances within the gimbaled suspension system are minimized, the antenna is properly guided and its axis remains stable, without unnecessary oscillations. In principle, stabilization is essentially a disturbance rejection problem [5, 6]. The main sources of disturbance include vibrations and angular and axial accelerations of the moving platform, as well as imbalances in the servo system and the rotating pedestal itself. Furthermore, geometric imperfections such as friction and mechanical imbalance exist even in optimally designed systems[7, 8]. These factors cause disturbance torques in the pedestal system, which must be adequately compensated [9]. The standard pedestal configuration consists of two rotational axes, Yaw and Pitch, and can serve as a reference model for other two-axis gimbal systems. Proper system balancing leads to a significant increase in antenna pointing accuracy. One of the main factors that contributes to control errors and increased power consumption in the motors is the effect of external acceleration forces acting on the pedestal structure [10]. Two standard test methods are used for simulated acceleration tests. One such technique is linear acceleration testing using centrifuge tables, following the guidelines provided in MIL-STD-810G, Method 513.6 [11, 12]. In contrast, the second technique involves sled rail testing, which is less commonly employed due to several limitations such as data transmission constraints (both sent and received signals) within the pedestal system, restricted testing space, and higher operational costs [13]. However, one advantage of the sled rail technique is that it avoids the rotational effects on the pedestal axes that are present in centrifuge-based testing. Rafał Lewkowicz et al. [14] presented an inverse kinematics model with three degrees of freedom and evaluated the effects of linear acceleration on various links of the system. Chen et al. [15] studied the kinematics, dynamics, and control algorithms of a centrifuge-based simulator, employing a three-joint model to control the motion of the centrifuge table. Dancuo et al. [16] presented a kinematic model for a human centrifuge table and studied the influence of contact accelerations on the system. Deng et al. [17] investigated the effects of aerodynamic and vibration forces on the main structural frame and motor mounting base of the setup. Wang et al. [18] performed a structural analysis to evalute how manufacturing and assembly errors affect the rotational accuracy of the centrifuge table. Numerous works have also focused on studying bearings and other structural support components in centrifuge test systems[19, 20], providing valuable insights into design considerations and mechanical performance [21, 22].

A review of the reviewed literature reveals that no prior work has been performed on the effects of centrifuge rotation on the dynamics of rotational axes within a two-degree-of-freedom pedestal or gimbal system. Accordingly, the focus of this study is dedicated to this subject. In this regard, the equations of motion are derived using the Lagrangian formulation. The centrifuge test is one of the key techniques for estimating the maximum torque of motors and is particularly effective in identifying imbalance within the system. For the first time, this test has also been employed on the prototype examined in this work.

2- Guidelines for Preparing Figures

The centrifuge system generates the required acceleration as a function of the rotational arm length, corresponding to the pedestal's mounting location, and the angular velocity. A schematic of the centrifuge test setup is shown in Fig. 1.

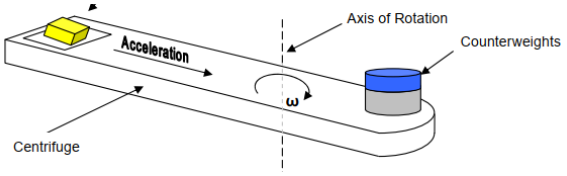

Fig.1. General schematic of the centrifuge platform [8]

As shown in Fig. 1, the device starts rotating with an increasing angular velocity and eventually reaches and maintains a constant target speed. As a result, a specific centrifugal acceleration is produced, governed by Eq. (1).

$$a_{centrifuge} = l\omega^2 \quad (1)$$

Here, l and ω represent the distance from the center of mass to the axis of rotation and the angular velocity of the table, respectively. In addition to providing an acceleration of 10g to evaluate imbalance and dynamic asymmetry (unbalance), angular velocity is also an important factor affecting the torque experienced by both motors in the pedestal. This presents a major challenge in centrifuge testing, as the required rotational speeds are considerably higher than those encountered in real-world operating conditions. In particular, under actual environmental and operating conditions of the vehicle, the angular velocity usually does not exceed 30 rpm. However, in the centrifuge test setup, given the 10g acceleration requirement and a limited arm length of less than 2 meters, the angular velocity should be approximately 50 rpm.

Fig. 2 demonstrates an overall view of the pedestal and its rotational axes. As shown in Fig. 2, the two axes are orthogonal and arranged in a Pitch-over-Yaw configuration. This means that, for modeling purposes, the Pitch axis rotates first, followed by the Yaw axis. Therefore, the rotation sequence is of critical importance. It should be noted, however, that this sequence does not imply that the two axes cannot move simultaneously.

Fig. 3 presents a two-degree-of-freedom (2-DOF) pedestal system mounted on the centrifuge stand. The figure shows two configurations of the rotation axis: one parallel to the Yaw axis, and the other perpendicular to it.

Fig. 4 shows the complete two-degree-of-freedom pedestal system, including all reference frames and coordinate axes.

The angles θ and ψ demonstrate the rotational angles in the Yaw direction associated with the larger motor axis, and the Pitch (or elevation) direction relative to the smaller motor axis, respectively, as also shown in Fig. 4. The pedestal motors are mounted along the z_1 and x_2 axes. The coordinate systems and notation are described in Table 1.

Table 1. Body-fixed and rotated coordinate systems

$(xyz)_0$	**Centrifuge body frame**
$(xyz)_1$	**θ: Rotation angle of the body frame (Yaw channel or azimuthal rotation)**
$(xyz)_2$	**ψ: Rotation angle of Frame 2 (Pitch channel or elevation rotation)**
(m_1, r_1)	**Mass and center of mass coordinates of Frame 1**
(m_2, r_2)	**Mass and center of mass coordinates of Frame 2**

The angular velocity of the antenna frames (outer frame, body 2), the inner frame (body 1), and the centrifuge associated with their respective reference frames is described as follows:

$$\omega_{0)0} = \begin{bmatrix} p \\ q \\ r \end{bmatrix},\ \omega_{1)1} = \begin{bmatrix} p_2 \\ q_2 \\ r_2 \end{bmatrix},\ \omega_{2)2} = \begin{bmatrix} p_3 \\ q_3 \\ r_3 \end{bmatrix} \quad (2)$$

$\omega_{i,j}$ demonstrates the angular velocity of body i expressed in the reference frame of body j, where q, p, and r are the components of the angular velocity along the Roll, Pitch , and Yaw directions, respectively.

The inertia matrix of the rotating frames is obtained as shown in Eq. (3).

$$I_1 = \begin{bmatrix} I_{x1} & I_{xy} & I_{xz} \\ I_{yx} & I_{y1} & I_{yz} \\ I_{zx} & I_{zy} & I_{z1} \end{bmatrix}, I_2 = \begin{bmatrix} I_{x2} & i_{xy} & i_{xz} \\ i_{yx} & I_{y2} & i_{yz} \\ i_{zx} & i_{zy} & I_{z2} \end{bmatrix} \quad (3)$$

As can be seen from Eq. (3), no negative signs appear in the inertia matrix. The off-diagonal elements of the inertia matrix demonstrate the cross-product terms of the mass inertia matrix.

The output of the system for the antenna or line-of-sight (LOS) is the angular velocities of body 2. Accordingly, the angular velocity of body 1 is obtained as follows:

$$\omega_{1)1} = \omega_{1/0)1} + \omega_{0)1} = [0 \quad 0 \quad \dot{\theta}]^T + {R_1}^T \omega_{0)0} \quad (4)$$

Similarly, the angular velocity of body 2 is obtained as:

$$\omega_{2)2} = \omega_{2/1)2} + \omega_{1/0)2} + \omega_{0)2} \quad (5)$$
$$= [\dot{\psi} \quad 0 \quad 0]^T + {R_2}^T [0 \quad 0 \quad \dot{\theta}]^T + {R_2}^T {R_1}^T \omega_{0)0}$$

In Eq.(5), $\omega_{0)0} = \begin{bmatrix} 0 \\ 0 \\ \dot{\alpha} \end{bmatrix}$. The terms $\dot{\alpha}$, $\dot{\psi}$, and $\dot{\theta}$ demonstrate rotational motions about the centrifuge axis, the pitch axis, and the yaw axis, respectively

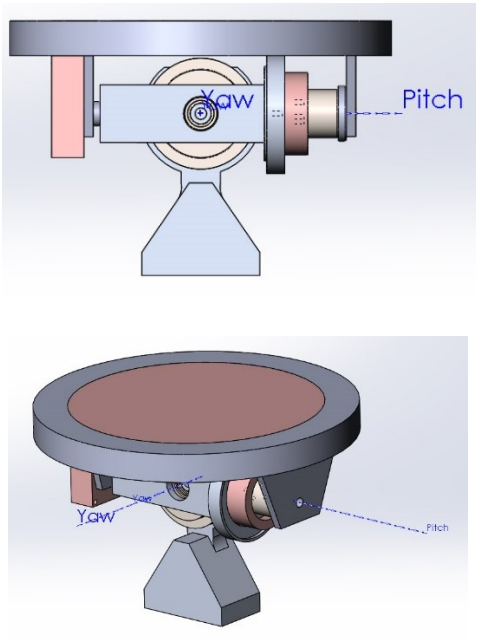

Fig.2. Overall view of the two-degree-of-freedom pedestal with Pitch and Yaw axes

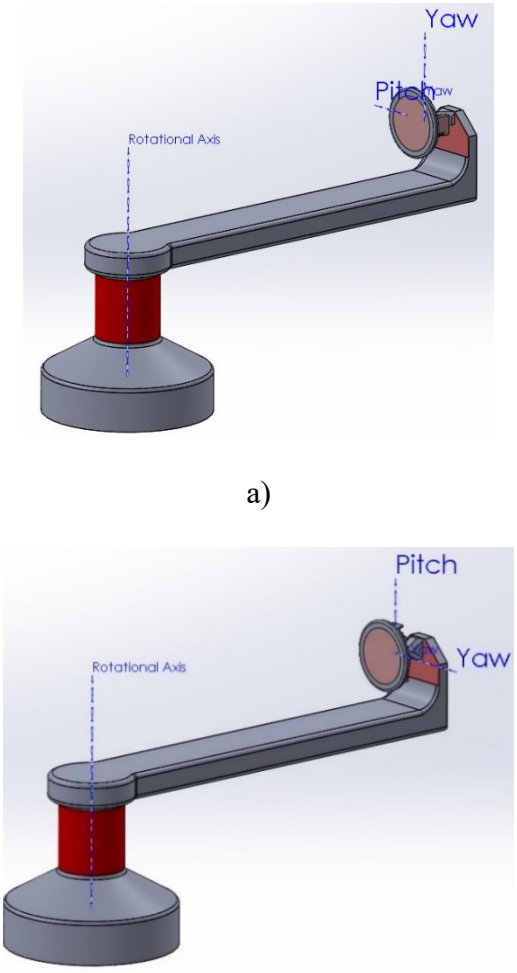

Fig.3. Two-degree-of-freedom pedestal mounted on the centrifuge table rotating about the Z and X axes: a) Centrifuge axis parallel to the Yaw axis, b) Centrifuge axis perpendicular to the Yaw axis

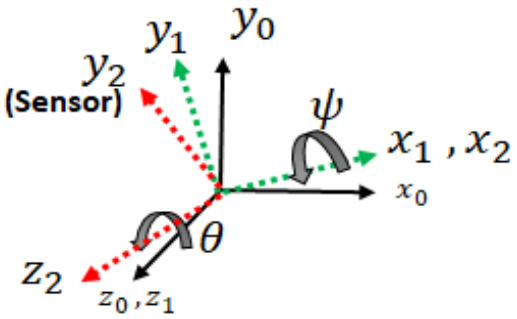

Fig. 4. The two-degree-of-freedom pedestal system with its associated coordinate systems

2.1-The velocity of the center of mass of each hoop or frame

The present work aims to investigate the effects of the intended centrifuge rotation. As a result, the effects of imbalance are ignored. The linear velocity of the center of mass of body 1 is given by:

$$V_{cg1)1} = {R_1}^T \omega_{0)0} \times r_0 \quad (6)$$

In Eq. (6), r_0 represents the position vector from the rotation axis to the center of rotation of the pedestal. Assuming that body 2 is mounted on the pitch axis and does not undergo translational motion, the linear velocity of its center of mass is obtained by:

$$V_{cg2)2} = {R_2}^T {R_1}^T \omega_{0)0} \times r_0 \tag{7}$$

To obtain the equations of motion, the Lagrange equation is used as follows:

$$Lagrangian = T - U \tag{8}$$

In Eq. (8), T and U represent the kinetic and potential energy of the three-degree-of-freedom simulator, respectively, as shown in Eq. (9).

$$\begin{aligned} T = {} & \frac{1}{2}{\omega_{1)1}}^T I_1 \omega_{1)1} + \frac{1}{2}{\omega_{2)2}}^T I_2 \omega_{2)2} + \frac{1}{2} m_1 {V_{1)1}}^T V_{1)1} \\ & + \frac{1}{2} m_2 {V_{2)2}}^T V_{2)2} U \\ & = m_1 {R_1}^T \vec{g}.r_1 + m_2 {R_2}^T {R_1}^T \vec{g}.r_2 \end{aligned} \tag{9}$$

Consequently, the Lagrange equations proceed as follows:

$$\begin{aligned} & \frac{d}{dt}\left(\frac{\partial L}{\partial \dot{\theta}}\right) - \frac{\partial L}{\partial \theta} = \frac{\partial \omega}{\partial \dot{\theta}}.T_z = T_z \\ & \frac{d}{dt}\left(\frac{\partial L}{\partial \dot{\psi}}\right) - \frac{\partial L}{\partial \psi} = \frac{\partial \omega}{\partial \dot{\psi}}.T_x = T_x \end{aligned} \tag{10}$$

The Lagrange equations for each frame are written in the coordinates of that frame, because the magnitude of a vector or any scalar quantity remains invariant in different coordinate systems. In general, the potential energy can be ignored because it is insignificant compared to the kinetic energy. A simplified form is employed to represent the rotating bodies as follows.

$$(xyz) \overset{R_1}{\rightarrow} (xyz)_1 \overset{R_2}{\rightarrow} (xyz)_2 \tag{11}$$

R_i is the transformation matrix that represents a rotated vector from frame i to frame i−1. Accordingly, R_i^T demonstrates a vector in frame i−1 expressed in the new frame i. The rotation matrices are obtained as follows

$$R_1 = \begin{bmatrix} c_\theta & -s_\theta & 0 \\ s_\theta & c_\theta & 0 \\ 0 & 0 & 1 \end{bmatrix} \tag{12}$$

$$R_2 = \begin{bmatrix} 1 & 0 & 0 \\ 0 & c_\psi & -s_\psi \\ 0 & s_\psi & c_\psi \end{bmatrix} \tag{13}$$

C and S denote the abbreviations for cosine and sine, respectively. The torque equations, in the absence of imbalance and assuming that the centrifuge axis of rotation is parallel to the Yaw axis, are given by:

$$\begin{aligned} T_z = {} & \left(\left(-I_{y2} + I_{z2}\right) cos\left(\Psi(t)\right)^2 + I_{y2} + I_{z1}\right)\left(\ddot{\theta}\right) \\ & + sin(2\Psi(t))\left(I_{y2} - I_{z2}\right)\dot{\Psi}\left(\dot{\theta} + \dot{\alpha}\right) \end{aligned} \tag{14}$$

$$T_x = I_{x2}\,\ddot{\Psi} - \frac{\sin\left(2\Psi(t)\right)\left(I_{y2} - I_{z2}\right)}{2}\left(\dot{\theta} + \dot{\alpha}\right)^2 \tag{15}$$

Here, T_x and T_z demonstrate the torques about the Pitch and Yaw axes, respectively. The Eqs. (14) and (15) define the behavior of the pedestal in the absence of imbalance, mounted on a centrifuge rotating at an angular velocity $\dot{\alpha}$ aligned with the z-axis, i.e., the azimuth axis. As seen, in all cases where under normal conditions (i.e., when the pedestal is not connected to the centrifuge assembly and there is no imbalance), the term $\dot{\theta}$ appears, it is replaced by $\dot{\theta} + \dot{\alpha}$. In other words, the angular velocity of the centrifuge is added to the angular velocity of the pedestal's azimuth axis. From Eqs. (14) and (15), two key factors emerge. The first is $\dot{\alpha}$, the angular velocity of the centrifuge, and the second is the term $\left(I_{y2} - I_{z2}\right)$, which appears repeatedly in both the current and subsequent equations. The closer this term is to zero, the smaller the additional torque becomes.

In the absence of any unbalance in all axes, and assuming that the center of mass of both rotating systems coincides with the center of rotation, no torque equations arise. In this study, an ideal balanced condition is intentionally assumed to isolate the pure influence of centrifuge rotation. Frictional and damping effects are not included because, under the pedestal stabilization mode, their variation with rotational speed is negligible and remains almost constant. Introducing unbalanced conditions at this stage would mask the primary effect of centrifuge-induced torque, which was the focus of the present analytical investigation. Furthermore, the centrifuge's axis of rotation is supposed to be perpendicular to the yaw axis.

$$\begin{aligned} & T_z \\ & = \left(\left(-I_{y2} + I_{z2}\right) cos\left(\Psi(t)\right)^2 + I_{y2} + I_{z1}\right)\left(\ddot{\theta}\right) \\ & + \left(I_{y2} - I_{z2}\right) sin\left(2\Psi(t)\right)\dot{\Psi}\dot{\theta} \\ & - \frac{sin\left(2\theta(t)\right)\left(\begin{matrix}\left(I_{y2} - I_{z2}\right) cos\left(\Psi(t)\right)^2 + \\ I_{y1} + I_{z2} - I_{x1} - I_{x2}\end{matrix}\right)}{2}\dot{\alpha}^2 \\ & - 2sin(\theta(t))\left(\left(I_{y2} - I_{z2}\right) cos\left(\Psi(t)\right)^2 + \frac{I_{z2} - I_{x2} - I_{y2}}{2}\right)\dot{\Psi}\dot{\alpha} \end{aligned} \tag{16}$$

$$\begin{aligned} & T_x \\ & = I_{x2}\,\ddot{\Psi} + \frac{\sin\left(2\theta(t)\right)\sin\left(\theta(t)\right)^2\left(I_{y2} - I_{z2}\right)}{2}\dot{\alpha}^2 \\ & + 2\,sin(\theta(t))\left(\begin{matrix}\left(I_{y2} - I_{z2}\right) cos\left(\Psi(t)\right)^2 \\ + \frac{I_{z2} - I_{x2} - I_{y2}}{2}\end{matrix}\right)\dot{\alpha}\dot{\theta} \\ & - \frac{\left(I_{y2} - I_{z2}\right) sin\left(2\Psi(t)\right)}{2}\dot{\theta}^2 \end{aligned} \tag{17}$$

In the torque equations of the pedestal on the centrifuge, under the condition where the centrifuge's rotation axis is parallel to the axis of yaw, the term $\dot{\alpha}^2$ appears in both the azimuth and elevation torque terms. Given the potentially high angular velocity of the centrifuge, this term can attain relatively large values and must be regulated employing appropriate coefficients, the most important of which is $\left(I_{y2} - I_{z2}\right)$, which should ideally be minimized or brought close to zero.

Considering real-world conditions in two-degree-of-freedom pedestals and various payload configurations such as antennas or cameras, as well as the structural configuration of the pitch axis, it seems unlikely that a pedestal can be designed in which the center of rotation of both rotating bodies coincides with the system's rotation axis. Therefore, it is necessary to investigate the torque equations in a scenario where no unbalance exists along any axis, but the centers of mass of both rotating subsystems do not coincide with the rotation center. As shown in Fig. 4, the center of mass of the pitch axis lies along the x-direction. For the yaw axis to be balanced, its center of mass must lie in the x–y plane. Assuming that the pitch axis is balanced in the z–y plane and the yaw axis is balanced along the y-axis, achieving balance in the x-direction for the yaw rotating body requires that the x-component of the pitch axis center of mass (x_2) be proportional to that of the yaw axis center of mass (x_1). Specifically, the condition $m_1 x_1 = m_2 x_2$ must be satisfied. For the sake of simplifying the equations, it is assumed that $m_1 = m_2$, and hence $x_1 = x_2$. Under these assumptions, and considering that the centrifuge's rotation axis is perpendicular to the yaw axis, the torque equations for both axes can be described as follows:

$$T_x = I_{x2}\,\ddot{\Psi} + \frac{\sin\left(2\theta(t)\right)\sin\left(\theta(t)\right)^2\left(I_{y2} - I_{z2}\right)}{2}\dot{\alpha}^2 \tag{18}$$

$$+2\,sin(\theta(t))\left(\begin{matrix}\left(I_{y2}-I_{z2}\right)cos\left(\Psi(t)\right)^2\\ +\frac{I_{z2}-I_{x2}-I_{y2}}{2}\end{matrix}\right)\dot{\alpha}\dot{\theta}$$

$$-\frac{\left(I_{y2}-I_{z2}\right)sin\left(2\Psi(t)\right)}{2}\dot{\theta}^2$$

$$T_z=\left(\left(-I_{y2}+I_{z2}\right)cos\left(\Psi(t)\right)^2+I_{y2}+I_{z1}+2mx^2\right)\left(\ddot{\theta}\right) \quad (19)$$

$$+\left(I_{y2}-I_{z2}\right)sin\left(2\Psi(t)\right)\dot{\Psi}\dot{\theta}$$

$$-\frac{sin\left(2\theta(t)\right)\left(\begin{matrix}\left(I_{y2}-I_{z2}\right)cos\left(\Psi(t)\right)^2+\\ I_{y1}+I_{z2}-I_{x1}-I_{x2}\end{matrix}\right)}{2}\boldsymbol{\dot{\alpha}^2}$$

$$-2sin\left(\theta(t)\right)\left(\left(I_{y2}-I_{z2}\right)cos\left(\Psi(t)\right)^2+\frac{I_{z2}-I_{x2}-I_{y2}}{2}\right)\dot{\Psi}\dot{\alpha}-mx^2sin\left(2\theta(t)\right)\dot{\alpha}^2$$

As seen in Eq. (18), the torque on the pitch axis, T_x, remains unchanged compared to Eq. (17), indicating that this configuration does not affect the pitch axis dynamics. However, comparing Eq. (19) for the yaw axis with Eq. (16), it is seen that the yaw torque, T_z, is modified by an additional term of $-mx^2sin\left(2\theta(t)\right)\dot{\alpha}^2$.

In addition, the coefficient of the angular acceleration $\ddot{\theta}$, which represents the moment of inertia about the yaw axis, increases by $2mx^2$. This correction is due to the parallel axis theorem, where the effective moment of inertia for systems with a center of mass offset from the rotation axis is given by $I_{axis}=I_{cg}+Mx^2$.

Considering only the centrifuge rotation condition, i.e., $\ddot{\theta}=\ddot{\Psi}=\dot{\theta}=\dot{\Psi}=0$, the equations become:

$$T_x=I_{x2}\,\ddot{\Psi}+\frac{\sin\left(2\theta(t)\right)\sin\left(\theta(t)\right)^2\left(I_{y2}-I_{z2}\right)}{2}\dot{\alpha}^2 \quad (20)$$

$$T_z \quad (21)$$

$$=\left(\left(-I_{y2}+I_{z2}\right)cos\left(\Psi(t)\right)^2+I_{y2}+I_{z1}\right)\left(\ddot{\theta}\right)$$

$$-\frac{sin\left(2\theta(t)\right)\left(\begin{matrix}\left(I_{y2}-I_{z2}\right)cos\left(\Psi(t)\right)^2+\\ I_{y1}+I_{z2}-I_{x1}-I_{x2}\end{matrix}\right)}{2}\boldsymbol{\dot{\alpha}^2}$$

$$-mx^2sin\left(2\theta(t)\right)\boldsymbol{\dot{\alpha}^2}$$

As shown in Eq. (21), under the actual centrifuge test conditions with the aforementioned assumptions, the mass and the x-direction position of the center of mass of both subsystems contribute to the torque around the yaw axis. This effect is non-negligible and must be taken into account. Therefore, during centrifuge tests, the term $-mx^2sin\left(2\theta(t)\right)\dot{\alpha}^2$ must be included in the evaluation.

3-Results and discussion

To evaluate and simulate the equations, a pedestal with ±60 degrees of rotational freedom in both axes is considered. The system assumes a diagonal inertia matrix with specified moments of inertia and a rotational speed of 100 RPM. The resulting torques applied to the pedestal motors are presented as a 3D plot concerning the angular positions ψ and θ (Theta–Psi).

The inertia matrices , related to the elevation and azimuth axes used in the simulations are explicitly defined as :

$$I_2=\begin{bmatrix}0.0009 & 0 & 0\\ 0 & 0.0025 & 0\\ 0 & 0 & .0024\end{bmatrix}(kg.m^2) \quad \text{and} \quad I_1=\begin{bmatrix}0.000054 & 0 & 0\\ 0 & 0.00032 & 0\\ 0 & 0 & .0003\end{bmatrix}(kg.m^2).$$

.The approximate physical dimensions of the pedestal are 18 × 18 × 15 cm. The products of inertia are of the order of 10^{-6} kg·m² and therefore negligible due to symmetry. The numerical parameters correspond to the characteristics of an actual centrifuge pedestal used in testing. A sensitivity analysis showed that proportional variations in the mass moments of inertia caused only marginal changes in torque results, confirming that the centrifugal effect is dominant. Moreover, if the geometric dimensions scale linearly, the induced centrifugal torque increases quadratically with the scale factor.

It is important to note that in the inertia matrix of subsystem 1, only components that rotate about the yaw axis are intended. As stated, the analysis focuses on the effect of the centrifuge. Consequently, to isolate the torque generated solely by this effect, all angular velocities and angular accelerations of the frames have been assumed to be zero, i.e., $\ddot{\theta}=\ddot{\Psi}=\dot{\theta}=\dot{\Psi}=0$. In the presented results, only the frame positions defined by the angles θ and ψ are considered as input variables.

Based on Fig. 3(a), under the condition where the yaw axis is parallel to the centrifuge rotation axis, and considering Eqs. (20) and (21), the resulting output torques as functions of the angles θ and ψ are presented in Figs. 5 and 6.

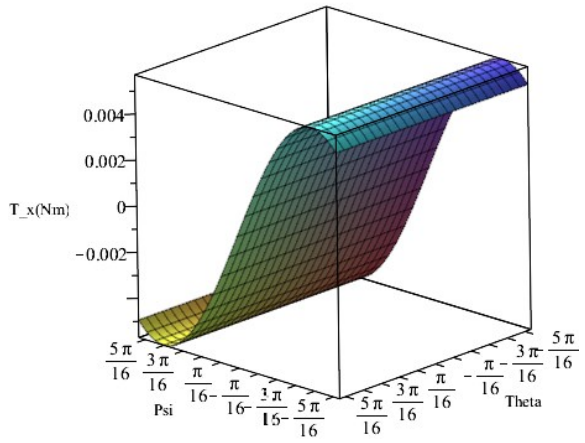

Fig. 5: Output torque of the pitch axis as a function of θ and ψ, for the case where the yaw rotation axis is parallel to the centrifuge rotation axis.

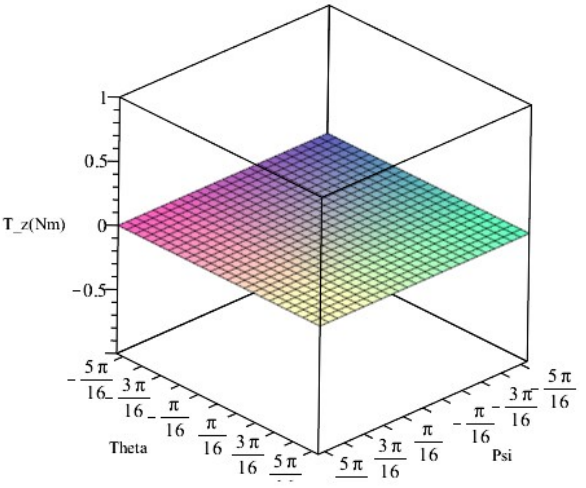

Fig. 6: Output torque of the yaw axis as a function of θ and ψ, for the case where the yaw rotation axis is parallel to the centrifuge rotation axis.

As shown in Fig. 5, no variation in torque concerning the angle θ is observed. This result is expected considering Eq. (20), as there is no term involving the variable θ in the equations.

In Fig. 6, the torque resulting from centrifuge rotation is zero at all angles, as the setting $\ddot{\theta} = \Psi \doteq 0$in Eq. (21) leads to zero output torque along this axis. Figure 6 demonstrates that, under the condition of parallel alignment between the two specified axes, no centrifuge-induced torque is exerted on this axis. Even in the presence of $\ddot{\theta}$and $\dot{\Psi}$ terms, the resulting torque is directly proportional to the first order of $\dot{\alpha}$, whereas for the pitch axis, the torque is directly proportional to the second order of $\dot{\alpha}$.

As observed in Fig. 5, the maximum torque value is 0.005 Nm. According to Fig. 3(a), under the condition of orthogonality between the two axes (the yaw axis and the rotation axis of the centrifuge) and based on Eqs. (16) and (17), the output torque results as a function of the angles θ and ψ are presented in Figs. 7 and 8.

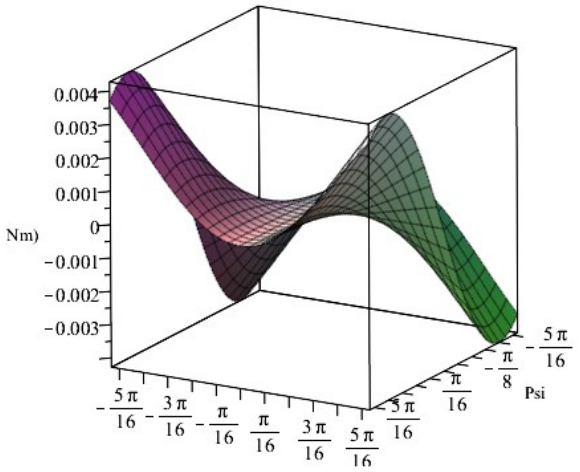

Fig. 7: Output torque of the pitch axis as a function of the angles θ and ψ for the case of orthogonality between the yaw rotation axis and the centrifuge rotation axis.

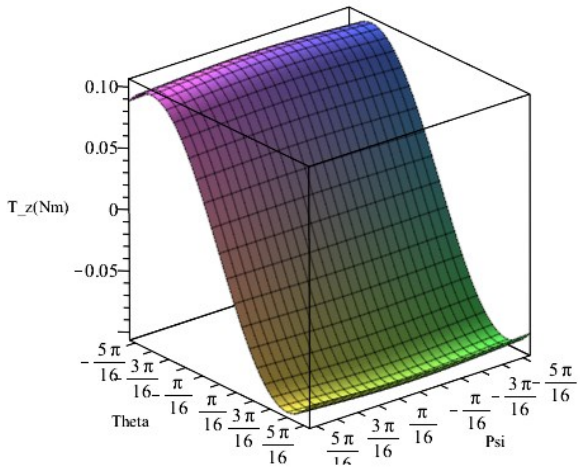

Fig. 8: Output torque on the yaw axis as a function of the angles θ and ψ for the case of orthogonality between the yaw rotation axis and the centrifuge rotation axis, under balanced conditions where the rotation axis aligns with the center of mass of each device.

As shown in Fig. 7, the maximum torque on this axis under the orthogonality condition between the two specified axes is approximately 0.004 Nm. The torque on the pitch axis is directly proportional to the second order of $\dot{\alpha}$. In Fig. 8, the maximum torque on the yaw axis is approximately 0.1 Nm. As indicated, the torque in this case is significantly higher for the yaw axis compared to the pitch axis. This high torque is due to its proportionality to the second order-of $\dot{\alpha}$ as well as the large difference in the moments of inertia in the yaw axis or rotating frame. It is important to note that the moment of inertia for the yaw axis is variable since changing the angle ψ\psiψ in the pitch axis alters the moments of inertia of the other two axes (excluding the primary rotation axis). In Eq. (17), the term $(I_{y2} - I_{z2})cos(\Psi(t))^2 + I_{y1} + I_{z2} - I_{x1} - I_{x2}$ represents the difference in the inertia matrix concerning the angle ψ in the yaw axis frame. As a result, one of the ways to reduce the effect of the centrifuge is to analyze and minimize the difference between the other two moments of inertia.

To better understand this concept, it is important to note that in rigid body dynamics, rotation about the principal axes is of critical importance. Principal axes are the axes that diagonalize the inertia matrix. If the body does not rotate about its principal axes, the angular velocity terms can have a significant impact on the resulting torque along the output axis.

$$I_1 = \begin{bmatrix} I_{xx} & 0 & 0 \\ 0 & I_{yy} & 0 \\ 0 & 0 & I_{zz} \end{bmatrix} \quad (22)$$

If the body does not rotate about a principal axis, a greater torque will be exerted on the motor axis (or the torque axis of interest). For one of the arbitrary axes, the following equation derived from rigid body dynamics applies [9]:

$$T_x = I_{x1}\dot{\omega}_x - \omega_y\omega_z(I_{yy} - I_{zz}) \quad (23)$$

As shown in Eq. (23), if the structure does not rotate solely about the principal axis (x), the term $\omega_y\omega_z$ will be nonzero. In cases where $(I_{yy} - I_{zz})$ is not zero—i.e., there is a significant difference in the moments of inertia along the other two axes (y and z)—the torque component T_x becomes larger. Consequently, the term $\omega_y\omega_z(I_{yy} - I_{zz})$, which arises from the centrifuge rotation, becomes dominant. As a result, the motor torque values, as reflected in the current draw, are inflated and do not represent the actual torque demand (i.e., they are misleading or "apparent" values). Based on the analysis of the equations and the resulting behavior, there are two feasible approaches to minimize the effect of the centrifuge. The first is to perform an acceleration test using a rail sled system, in which case the centrifuge effect is eliminated. The second is to add a counter-rotating system to the centrifuge arm that applies a rotational velocity opposite to that of the centrifuge, allowing only the effect of linear acceleration to be observed. Aside from these two approaches, the only option is to account for this effect analytically and subtract it from the measured output torque.

Based on the results shown in Fig. 8, it can be concluded that the effect of centrifuge rotation on the yaw axis is highly significant. To investigate the effects of rotational acceleration of the centrifuge device on the yaw axis, the torque analysis and the influence of realistic balancing conditions for the yaw axis are examined. For these conditions, it can be assumed that the entire rotating pitch system has a mass of $m_2 = 0.75\ kg$, and the yaw rotating system (exclusively) has a mass of $m_1 = 0.25\ kg$. By examining the effects of balancing on the yaw axis, it is observed that with an increase in mass in both axes, as well as an increase in x_2 andx_1, the torque on the yaw axis varies considerably. This occurs despite the yaw axis being fully balanced, where it would be expected that, under the condition of maintaining balance on the yaw axis (i.e., proportional mass distribution along the x-direction), there would be no change in torque. Figs. 9 through 11 illustrate the yaw axis torque values under various positions of the centers of mass of the two rotating frames along the x-axis, while maintaining balance on the yaw axis.

The three cases examined are as follows:

- Mass $m_2 = 0.75\,Kg$ with the center of mass located at $x_2 = 5mm$ in the pitch frame.
- Mass $m_2 = 0.75\,Kg$ with the center of mass located at $x_2 = 10mm$ in the pitch frame.
- Mass $m_2 = 0.75\,Kg$ with the center of mass located at $x_2 = 15mm$ in the pitch frame.

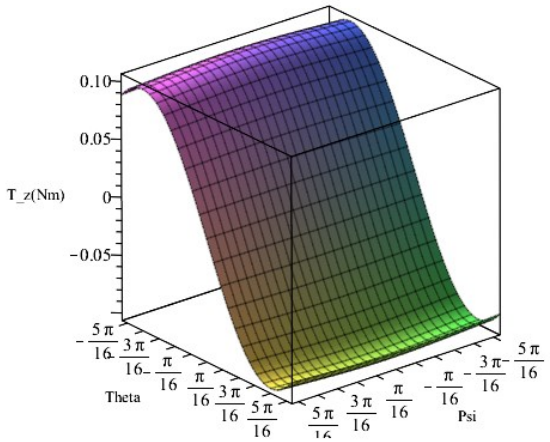

Fig. 9: Output torque on the yaw axis as a function of the angles θ and ψ for the case of orthogonality between the yaw rotation axis and the centrifuge rotation axis, under balanced conditions but with misalignment between the rotation axis and the center of mass of each device ($x_2 = 5mm$).

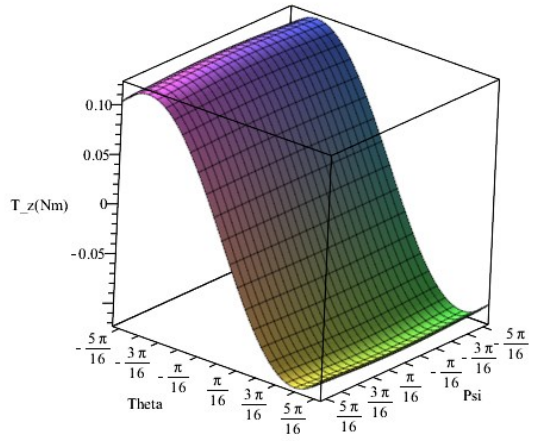

Figure 10: Output torque on the yaw axis as a function of the angles θ and ψ for the case of orthogonality between the yaw rotation axis and the centrifuge rotation axis, under balanced conditions but with misalignment between the rotation axis and the center of mass of each device ($x_2 = 10mm$).

As shown in Fig. 9, the variation in maximum torque compared to the conditions in Fig. 8 is approximately 0.005 Nm, indicating that the offset of the pitch system's center of mass has had a minimal effect. This is due to the small value of $x_2 = 5mm$. However, in Fig. 10, the variation in maximum torque compared to Fig. 8 is approximately 0.02 Nm, and in Fig. 11, the variation reaches approximately 0.045 Nm. According to Eq. (17), which includes the term $mx^2 sin(2\theta(t))\dot{\alpha}^2$, it can be observed that the torque increases proportionally with the square of $x_2 = x$. Therefore, the increase in torque from 0.005 Nm to 0.045 Nm is consistent with the quadratic relationship and is entirely valid.

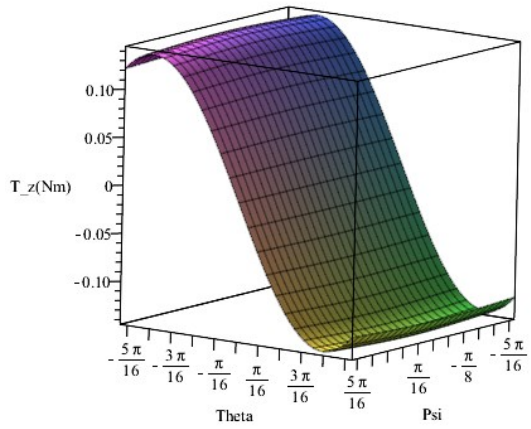

Fig. 11: Output torque on the yaw axis as a function of the angles θ and ψ for the case of orthogonality between the yaw rotation axis and the centrifuge rotation axis, under balanced conditions but with misalignment between the rotation axis and the center of mass of each device ($x_2 = 15mm$).

All figures were plotted using raw simulation outputs without any normalization. Therefore, they mainly demonstrate the qualitative trend of the torque variations with the centrifuge rotation parameters rather than absolute magnitudes. Future work will include a quantitative comparison between the simulated torque values and typical actuator and motor torque limits using the same experimental prototype.

The results of this section demonstrate, for the first time, that the rotational motion of the centrifuge table has a significant impact on the rotating axes in tracking pedestals (or similar systems), and in some cases, can lead to a substantial increase in the motor torque requirements. This effect can be mitigated by increasing the arm length of the centrifuge table during installation. As shown in the equations, the torque consumption is directly proportional to the square of the centrifuge table's rotational rate, and therefore, its effects must be carefully considered in system design and analysis.

4-Conclusion

In this study, the effect of centrifuge table rotation on the dynamics of two-degree-of-freedom bases used in tracking mechanisms was analytically and numerically investigated for the first time. Contrary to conventional approaches that primarily consider only the linear acceleration induced by the centrifuge, this paper demonstrates that the rotation of the centrifuge table itself can introduce unexpected and disturbing torques on the gimbal axes (Pitch and Yaw). These torques arise not only under specific conditions but also in configurations where the system is fully balanced, and they are strongly dependent on the angular velocity of the table and the location of the components' center of mass.

To accurately analyze this phenomenon, Lagrangian modeling was employed, and the effect of centrifuge rotation was evaluated in two distinct scenarios—when the centrifuge rotation axis is either parallel or perpendicular to the Yaw axis. Simulation results indicated that the apparent torques generated can lead to significant misestimations of the motor power requirements and dynamic behavior of the system unless properly modeled and compensated for. Based on the conducted analyses, design modifications—such as increasing the length of the centrifuge's rotating arm or implementing compensatory systems—alongside the use of precise analytical assessments prior to physical testing, can effectively prevent critical errors in the design and evaluation of mechanical systems.

In summary, the results of this study elucidate several key innovations in the field of dynamic testing of two-degree-of-freedom bases using centrifuges:

- For the first time, the effect of centrifuge table rotation on the dynamic torques applied to the gimbal axes was investigated.
- Precise Lagrangian equations were developed for two distinct configurations: with the Yaw axis parallel and perpendicular to the rotation axis.
- It was demonstrated that misalignment of the center of mass in rotating systems can generate non-negligible torques even under fully balanced mass conditions.
- The analysis revealed how differences in moments of inertia about non-principal axes amplify the rotational effects.
- As mitigation strategies, methods such as increasing the centrifuge arm length, employing counter-rotation systems, and analytically modeling and subtracting apparent torques were proposed.
- It was conclusively shown that torques resulting from centrifuge rotation can lead to significant errors in estimating the actual torque requirements of the system during testing.

- Given the column width of the article, the width of the figures must be 75 mm. If a larger image is necessary, the width must be 160 mm (i.e., the width of two columns).
- All numbers and labels within the figures must be legible, and the font size and elements should be proportionate to each other and consistent with the main text.
- A uniform and consistent style should be maintained across all figures in the article.
- For multi-part figures (e.g., parts a, b, etc.), the layout should follow a left-to-right arrangement.
- If figures are taken from software such as SolidWorks, Abaqus, etc., ensure that the background of the images is white.

Declaration of interests

The authors declare that they have no known competing financial interests or personal relationships that could have appeared to influence the work reported in this paper.

Funding Declaration

No funding

Ethics Approval

The scientific content of this article is the result of the authors' research and has not been published in any Iranian or international journal.

References

[1] Y. Wang, S. Zhao, J. Wu, L. Tan, P. Dong, and C. Zhang, "Sampled-data self-learning observer based attitude tracking control against sensor-actuator faults," *Aerospace Systems,* pp. 1-13, 2025. doi:10.1007/s42401-025-00341-5

[2] K. Qiu, H. Zhang, J. Zhang, R. Xiong, H. Lu, and Y. Wang, "An actuator space optimal kinematic path tracking framework for tendon-driven continuum robots: Theory, algorithm and validation," *The International Journal of Robotics Research,* p. 02783649241290525, 2024. doi:10.1177/02783649241290525

[3] Y. Xia, Q. Bao, and Z. Liu, "A new disturbance feedforward control method for electro-optical tracking system line-of-sight stabilization on moving platform," *Sensors,* vol. 18, no. 12, p. 4350, 2018. doi:10.3390/s18124350

[4] I. Naderi, D. E. Dickerson, and M. Ashrafi, "DEVELOPING A METHODOLOGY TO EXAMINE THE ROLE OF PROJECT CONTRACTS MANAGEMENT AS A PRECURSOR TO MANAGE PROJECTS," in *Proceedings of the International Annual Conference of the American Society for Engineering Management.*, 2024, pp. 1-6: American Society for Engineering Management (ASEM).

[5] Y. Sun, F. Zhao, Z. Guo, and X. Yan, "Dynamic modeling and parameters optimization of parallel–suspension type inertially stabilized platform," *Proceedings of the Institution of Mechanical Engineers, Part C: Journal of Mechanical Engineering Science,* vol. 239, no. 7, pp. 2357-2382, 2025. doi:10.1177/09544062241296393

[6] J. Tayebi, Y. Chen, T. Chen, and S. Jia, "Attitude control of flexible satellite via three-dimensional magnetically suspended wheel," *Applied Mathematics and Mechanics,* vol. 46, no. 3, pp. 555-572, 2025. doi: 10.1007/s10483-025-3232-7

[7] J. P. Mo, *Proceedings of the 10th International Conference on Mechanical, Automotive and Materials Engineering: CMAME 2023, 20–22 December, Da Nang, Vietnam*. Springer Nature, 2024. doi:10.1007/978-981-97-4806-8

[8] I. Naderi and D. E. Dickerson, "Evaluating the Influence of Project Contracts on Project Scheduling: A Novel Perspective," in *IISE Annual Conference. Proceedings*, 2025, pp. 1-6: Institute of Industrial and Systems Engineers (IISE). https://doi.org/10.21872/2025IISE_6959

[9] W. Ren *et al.*, "Stabilization control of electro-optical tracking system with fiber-optic gyroscope based on modified smith predictor control scheme," *IEEE Sensors Journal,* vol. 18, no. 19, pp. 8172-8178, 2018.

[10] J. M. Hilkert, G. Kanga, and K. Kinnear, "Line-of-sight kinematics and corrections for fast-steering mirrors used in precision pointing and tracking systems," in *Airborne Intelligence, Surveillance, Reconnaissance (ISR) Systems and Applications XI*, 2014, vol. 9076, pp. 115-129: Spie. doi:10.1117/12.2049857

[11] D. M. Nagle, G. J. Roesser, and T. Wilhelm, "Test Methods for Multi-Axis Simulation Testing per MIL-STD-810G," SAE Technical Paper0148-7191, 2010. doi:10.4271/2010-01-0284

[12] I. Naderi, D. E. Dickerson, and M. Ashrafi, "From Crisis to Strategy and Action: A Qualitative Study to Understand the Impact of COVID-19 on Implementing Knowledge Management in Organizations," in *IISE Annual Conference.*

Proceedings, 2024, pp. 1-6: Institute of Industrial and Systems Engineers (IISE). https://doi/10.21872/2024IISE_6691

[13] S. Walia, V. Satya, S. Malik, S. Chander, S. Devi, and A. Sharma, "Rocket Sled Based High Speed Rail Track Test Facilities: A Review," *Defence Science Journal,* vol. 72, no. 2, 2022. doi:١٠,١٤٢٩dsj.72.17014

[14] R. Lewkowicz and G. Kowaleczko, "An inverse kinematic model of the human training centrifuge motion simulator," *Journal of Theoretical and Applied Mechanics,* vol. 57, 2019. Doi:10.15632/jtam-pl.57.1.99

[15] Y.-C. Chen and D. Repperger, "A study of the kinematics, dynamics and control algorithms for a centrifuge motion simulator," *Mechatronics,* vol. 6, no. 7, pp. 829-852, 1996. doi:10.1016/09574158(96)00018-9

[16] Z. Dančuo, B. Rašuo, J. Vidaković, V. Kvrgić, and M. Bućan, "On Mechanics of a High-G Human Centrifuge," *Pamm,* vol. 13, no. 1, pp. 39-40, 2013. doi:10.1002/pamm.201310015

[17] C. Deng, L. He, Z. Tan, and X. Jia, "Vibration and Aerodynamic Analysis and Optimization Design of a Test Centrifuge," *Vibration,* vol. 6, no. 4, pp. 917-931, 2023. doi:10.3390/vibration6040054

[18] H. B. Z. Wang, Y.M.; Li, F. , " Influence of structure error on the rotary precision of precision centrifuge," *Equip. Environ. Eng,* vol. 12, pp. 72–77, 2015.

[19] R. Kostek, "Simulation and analysis of vibration of rolling bearing," *Key Engineering Materials,* vol. 588, pp. 257-265, 2014. doi:10.4028/www.scientific.net/KEM.588.257

[20] A. K. Rue, "Stabilization of precision electrooptical pointing and tracking systems," *IEEE Transactions on Aerospace and Electronic Systems,* no. 5, pp. 805-819, 1969. doi:10.1109/TAES.1969.309879

[21] G. Wang and M.-l. Guo, "Stiffness of aerospace rolling bearings," *Harbin Gongye Daxue Xuebao(Journal of Harbin Institute of Technology),* vol. 33, no. 5, pp. 644-645, 2001. doi:10.3390/lubricants10060116

[22] Y. Liu, C. Yan, J. Kang, Z. Wang, and L. Wu, "Investigation on characteristics of vibration interaction between supporting bearings in rotor-bearing system," *Measurement,* vol. 216, p. 113000, 2023. doi:10.1016/j.measurement.2023.113000

.